analytical chemistry

pubs.acs.org/ac Article

High-Temporal-Resolution smFISH Method for Gene Expression Studies in *Caenorhabditis elegans* Embryos

Seleipiri Charles,[⊥] Guillaume Aubry,[⊥] Han-Ting Chou, Annalise B. Paaby, and Hang Lu*

Cite This: *Anal. Chem.* 2021, 93, 1369−1376 Read Online

ACCESS | Metrics & More | Article Recommendations | Supporting Information

ABSTRACT: Recent development in fluorescence-based molecular tools has contributed significantly to developmental studies, including embryogenesis. Many of these tools rely on multiple steps of sample manipulation, so obtaining large sample sizes presents a major challenge as it can be labor-intensive and time-consuming. However, large sample sizes are required to uncover critical aspects of embryogenesis, for example, subtle phenotypic differences or gene expression dynamics. This problem is particularly relevant for single-molecule fluorescence in situ hybridization (smFISH) studies in *Caenorhabditis elegans* embryogenesis. Microfluidics can help address this issue by allowing a large number of samples and parallelization of experiments. However, performing efficient reagent exchange on chip for large numbers of embryos remains a bottleneck. Here, we present a microfluidic pipeline for large-scale smFISH imaging of *C. elegans* embryos with minimized labor. We designed embryo traps and engineered a protocol allowing for efficient chemical exchange for hundreds of *C. elegans* embryos simultaneously. Furthermore, the device design and small footprint optimize imaging throughput by facilitating spatial registration and enabling minimal user input. We conducted the smFISH protocol on chip and demonstrated that image quality is preserved. With one device replacing the equivalent of 10 glass slides of embryos mounted manually, our microfluidic approach greatly increases throughput. Finally, to highlight the capability of our platform to perform longitudinal studies with high temporal resolution, we conducted a temporal analysis of *par-1* gene expression in early *C. elegans* embryos. The method demonstrated here paves the way for systematic high-temporal-resolution studies that will benefit large-scale RNAi and drug screens and in systems beyond *C. elegans* embryos.

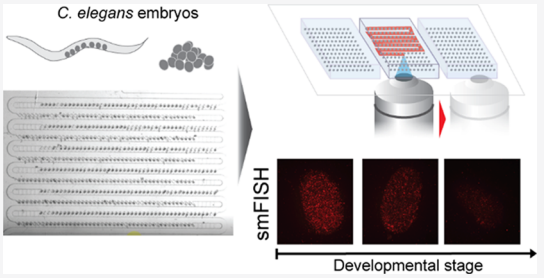

Small genetic model organisms, such as *Caenorhabditis elegans* and *Drosophila melanogaster*, have been used to address many questions in organismal development.[1−3] Technical advancements such as CRISPR, single-molecule fluorescence in situ hybridization (smFISH), and super-resolution microscopy have contributed significantly to biological discoveries.[4−9] Many of the readouts of these studies rely on the visualization of cell-biological events using fluorescence-enabled methods, as fluorescent markers can quantitatively report molecular positions and numbers with reasonable precision. The challenge with fluorescence reporters, especially nongenetically encoded reporters, is that they tend to involve many steps of manipulating the specimen to obtain a clear signal, e.g., washing, hybridizing, staining, and blocking. On the other hand, direct staining and hybridizing methods permit the treatment of multiple genotypes, an experimental design often required in evolutionary developmental biology and quantitative genetics. However, such studies typically also require large sample sizes for statistical reasons, and these multistep experiments do not scale well in terms of manual labor and time involved. As a result, this technical limitation creates a bottleneck in addressing any questions requiring high replication, such as phenotypic differences between wild-type genotypes from a natural population or dynamic changes in gene expression over developmental time. This hampers the application of tools of developmental genetics to systems biology.

This problem is particularly relevant when using smFISH to study gene expression changes during *C. elegans* embryogenesis. smFISH is a broadly used technique that allows for counting individual mRNA molecules by targeting a gene of interest using short nucleic acid probes with a fluorescent label.[10,11] Many smFISH-based techniques have been recently developed to increase the versatility of this approach and make smFISH a powerful tool for studying the spatiotemporal expression of genes.[12−17] However, smFISH implementation in embryogenesis studies remains difficult. For example, when targeting a specific developmental stage or performing longitudinal studies in *C. elegans*, rapid cell division makes isolating embryos of a particular stage of interest an inefficient process (Figure 1A). In addition, tens of individual samples are often required to account for heterogeneity in gene expression,

Received: July 12, 2020
Accepted: December 8, 2020
Published: December 23, 2020

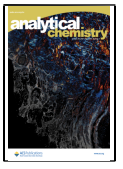

https://dx.doi.org/10.1021/acs.analchem.0c02966
Anal. Chem. 2021, 93, 1369−1376

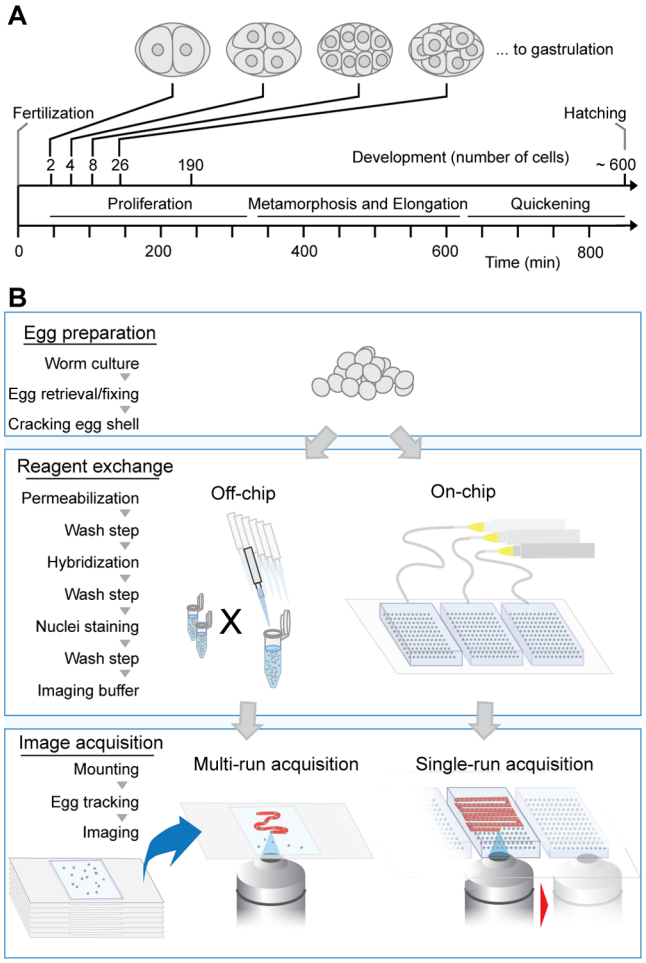

Figure 1. Pipeline for studying gene expression during embryogenesis with high temporal resolution. (A) Timeline of early-stage development of *C. elegans* embryos. (B) Schematic highlighting advantages of our integrated microfluidic pipeline vs traditional off-chip method for smFISH imaging: parallelization of experiments and automated imaging.

resulting in the need to process hundreds of embryos per experimental condition. Performing such an assay is arduous due to the complexity of smFISH protocols that are time-consuming and labor-intensive. This issue becomes even more exacerbated as the number of experimental conditions increases to study mutants, natural variants, or different treatments. Therefore, an effective platform to broaden the impact of the smFISH method for embryogenesis studies would require single-embryo resolution, capability of assaying hundreds of embryos simultaneously, and parallelization of the protocol. Furthermore, resolving these issues would also enhance many other imaging techniques that require multiple reagent exchange steps.

Microfluidics has the potential to transform smFISH into a high-throughput technique for *C. elegans* embryogenesis studies. Previous studies have demonstrated the use of microfluidic devices to array *C. elegans* embryos.[18−21] However, these devices have a limited capacity (~100 traps per array) due to low density of traps per area. In addition, these devices are designed specifically for live imaging with no need for reagent exchange. Integrating reagent exchange on-chip is nontrivial due to the presence of many flow perturbations during the protocol that can lead to sample movement and sample loss. Since many imaging-based techniques require multiple reagent exchanges, there is an acute need for microfluidic devices for handling a large amount of samples, allowing parallelization, and obtaining complementary information via combining several of these techniques. Establishing a pipeline that allows for efficient reagent exchange without losing embryos remains challenging and would enable a broad range of molecular tools to be applied to developmental systems biology.

Here, we present a microfluidic pipeline to address this challenge. We designed embryo traps and established a protocol capable of staining hundreds of *C. elegans* embryos simultaneously with efficient reagent exchange. We applied this process to a multistep smFISH protocol. Using smFISH probes targeting the embryonic gene *par-1*, we show that the on-chip smFISH protocol allows for parallelization of experiments while preserving image quality relative to the traditional slide-based method, thus enabling high temporal resolution of gene expression during early embryogenesis. Our microfluidic smFISH pipeline is thus a powerful tool for characterizing the dynamics of gene expression changes during embryogenesis.

EXPERIMENTAL SECTION

Microfluidic Device Fabrication. The microfluidic device was fabricated using soft lithography.[22] Briefly, the master was obtained via successive optical lithography steps using SU-8 2015 and SU-8 2025 photoresists (MicroChem) onto a silicon wafer. The channel depths were 12 μm for the backflow channel and 50 μm for the rest of the network. After development in SU-8 developer, the master was treated overnight with tridecafluoro-1,1,2,2-tetrahydrooctyl-1-trichlorosilane vapor (Sigma-Aldrich). A mixture of 10:1 poly(dimethylsiloxane) (PDMS): cross-linker was then poured on top of the wafer to obtain a thickness of ~5 mm and cured in an oven at 70 °C for 48 hours. Then, blocks of PDMS were cut, access wells were punched, and the PDMS blocks were bonded to coverslips via plasma treatment. Scaling-up via multiarray integration was achieved by bonding several devices on the same glass slide.

***C. elegans* Maintenance and Reagents.** N2 strain nematodes were grown on NGM agar plates with OP50 *Escherichia coli* lawns at 20 °C. Bleaching solution, M9 buffer solutions were prepared as previously described;[23] surfactant Tween 20 (Sigma-Aldrich) was mixed in M9 solution at 0.03% (w/w). The fixation buffer was composed of 5 mL of 37% formaldehyde (Sigma-Aldrich) and 45 mL of nuclease-free PBS 1× (Corning). Ethanol was mixed in deionized water at 70%. 4′,6-Diamidino-2-phenylindole (DAPI) staining solution was used to stain chromosomes and identify cell nuclei. Custom-made dry smFISH probes (Stellaris) targeting *par-1* labeled with Quasar 670 were dissolved in TE buffer (10 mM Tris−HCl, 1 mM EDTA, pH 8.0). The final hybridization buffer is composed of 1 g of dextran sulfate, 1 mL of 20× saline-sodium citrate (SSC), nuclease-free, 1 mL of deionized formamide, 8 mL of nuclease-free water, and 1.25 μM of the smFISH probe.

Wash buffer was made from 10% formamide, 2× SSC, in nuclease-free water. Prior to imaging, embryos were prepared with GLOX antifade buffer (850 μL of nuclease-free water, 40 μL of 10% glucose in water, 10 μL of 1 M Tris−HCl, pH 8.0, 100 μL of 20× SSC), followed by GLOX buffer with enzymes. The solution of GLOX buffer with enzymes was obtained using 100 μL of GLOX buffer and 1 μL of catalase solution and 1 μL

https://dx.doi.org/10.1021/acs.analchem.0c02966
Anal. Chem. 2021, 93, 1369−1376

of glucose oxidase solution. The catalase solution is composed of catalase from *Aspergillus niger* at ≥4000 U/mg protein in ammonium sulfate suspension (Sigma-Aldrich, C3515). The glucose oxidase solution is composed of glucose oxidase from *A. niger* (Sigma-Aldrich, G2133) at 3.7 mg/mL in 50 mM sodium acetate solution. For the flow-visualization experiments, fluorescein isothiocyanate (FITC)-dextran was dissolved in hybridization buffer at 1 mg/mL.

smFISH Protocol On Chip. Embryos were obtained by bleaching gravid-adult animals[23] and immediately transferred into microcentrifuge tubes filled with a 1 mL fixation buffer. After 15 min on a rotary shaker, the tubes were submerged in liquid nitrogen for 2 min to freeze-crack the embryo shells, then thawed in running water, and placed on ice for 20 min. The resulting pellet was washed and resuspended in M9 solution with surfactant at roughly 10,000 embryos per mL. The embryos were then manually loaded into the device using a syringe. All subsequent reagents were delivered from the side inlet of the device via a syringe. For every reagent change, the inlet tubing is clipped before releasing pressure from the syringe. Then, a new syringe containing the next reagent is connected. Finally, gentle positive pressure is applied to the new syringe while the inlet tubing is unclipped. The devices were continuously perfused with 70% ethanol overnight at 4 °C using a flow rate of 125 μL/h.

The on-chip smFISH protocol was developed from previously published techniques for *C. elegans* embryos.[10,11] All wash steps were conducted at 900 μL/h, while incubation steps were conducted by flowing at 500 μL/h for 10 min every 30−60 min. Following the overnight permeabilization in 70% EtOH, the embryos were washed in wash buffer for 10 min before incubation in hybridization buffer at 37 °C for 4 h. Next, the embryos were washed with wash buffer for 30 min and stained with DAPI for 45 min. The hybridization, wash, and DAPI staining steps were conducted in the dark. Finally, the samples were washed with wash buffer, 2× SSC, and then GLOX antifade buffer followed by GLOX buffer containing enzymes before proceeding to imaging.

smFISH Protocol Off Chip. The same reagents were used for on- and off-chip experiments. The embryo preparation up to freeze-cracking was identical to the on-chip protocol. Afterward, the embryos in the microcentrifuge tube were resuspended in 70% ethanol and rotated overnight at 4 °C. Reagent exchange off-chip was carried out by spinning down the embryos for 30 s using a centrifuge, removing the supernatant, and resuspending the embryos in a new reagent. Embryos were mounted on glass coverslips and using Glox antifade buffer.

Fluorescence Microscopy and Signal Quantification. All smFISH images were obtained using a spinning disk confocal microscope (Perkin Elmer UltraVIEW VoX) equipped with a Hamamatsu C9100-23b back-thinned EM-CCD and a 100× oil immersion objective. The smFISH images were analyzed using FISH-quant software to identify and count the punctae.[24] To enable accurate comparisons between on-chip and off-chip samples, we matched the age of the embryos and the sample size for each experiment. Signal-over-noise ratio (SNR) and signal-over-background ratio (SBR) are calculated using a custom MATLAB code. Briefly, after masking the embryo area, 2-Gaussian fit modeling was applied to the pixel intensity distribution to identify the background and punctae. The mean of the "punctae" Gaussian was used to threshold the embryo image and split the image into a background-only image and a punctae-only image. The peak amplitudes of all distinct areas of the punctae image were averaged to obtain the signal amplitude A. The background image was processed to obtain its mean, B, and standard deviation, N, to characterize the background level and noise. SNR and SBR were quantified using the equations $\mathrm{SNR} = (A - B)/N$ and $\mathrm{SBR} = A/B$.

For the flow-visualization experiments, we flowed the FITC dye solution from the side inlet at a flow rate of ∼500 μL/h on a dissecting scope (Leica, MZ16F). We quantified the dynamics of fluorescence intensity in the microchannels using a custom MATLAB code.

EXPERIMENTAL DESIGN

We aimed to create a pipeline that considerably increases the throughput of smFISH, maximize sample size, and thus improve the temporal resolution of gene expression during embryonic development. smFISH protocols are complex; they include sample collection, fixation, membrane permeabilization, staining, and mounting for imaging. Altogether, 10 steps are necessary to treat the embryos and prepare them for imaging in traditional smFISH. Figure 1B shows an overview of our method in parallel to the off-chip protocol to highlight some of the advantages of our pipeline. Using a microfluidic device enables the arraying of hundreds of embryos while allowing for reagent exchange necessary to the execution of the smFISH protocol. The on-chip pipeline allows for increasing throughput during imaging. Using a high-density array for embryo ordering and trapping, we minimize the painstaking task of preparing numerous single glass slides and circumvent the need for a user to set up each glass slide one after the other during the imaging session. Using our microfluidic approach, image acquisition can be performed in one run with minimal input from the user.

RESULTS AND DISCUSSION

Designing Platform for Large-Scale Arraying and smFISH Analysis of *C. elegans* Embryos. To study gene expression during embryogenesis requires assaying embryos at specific developmental stages. Precise monitoring of developmental stage is important as gene expression can vary rapidly. However, achieving temporal resolution is difficult because developmental stages can only be determined post analysis and hundreds of embryos may need to be processed to capture the desired stages. Indeed, cell divisions in early embryogenesis, up to gastrulation, occur every few minutes after fertilization and take place before the embryos are normally laid outside the body; the zygote then transforms into a 300-cell embryo within 300 min and hatches into a nearly 600-cell larva within 850 min[25] (Figure 1A). The rapid development process makes data acquisition challenging, particularly for early embryonic stages. Assuming a 5−10% efficiency to collect embryos of a given stage and the need for a few tens of data points to capture gene expression variation, establishing representative gene expression in early embryogenesis requires collecting approximately 300−500 embryos. To arrange such a large number of embryos on a single glass slide is a challenging task because the embryos must remain separated to ensure quality readout. Performing this step in a time-effective manner is important too. The whole smFISH protocol requires several days; one wants to complete this preparatory step within a few minutes to minimize labor.

https://dx.doi.org/10.1021/acs.analchem.0c02966
Anal. Chem. 2021, 93, 1369−1376

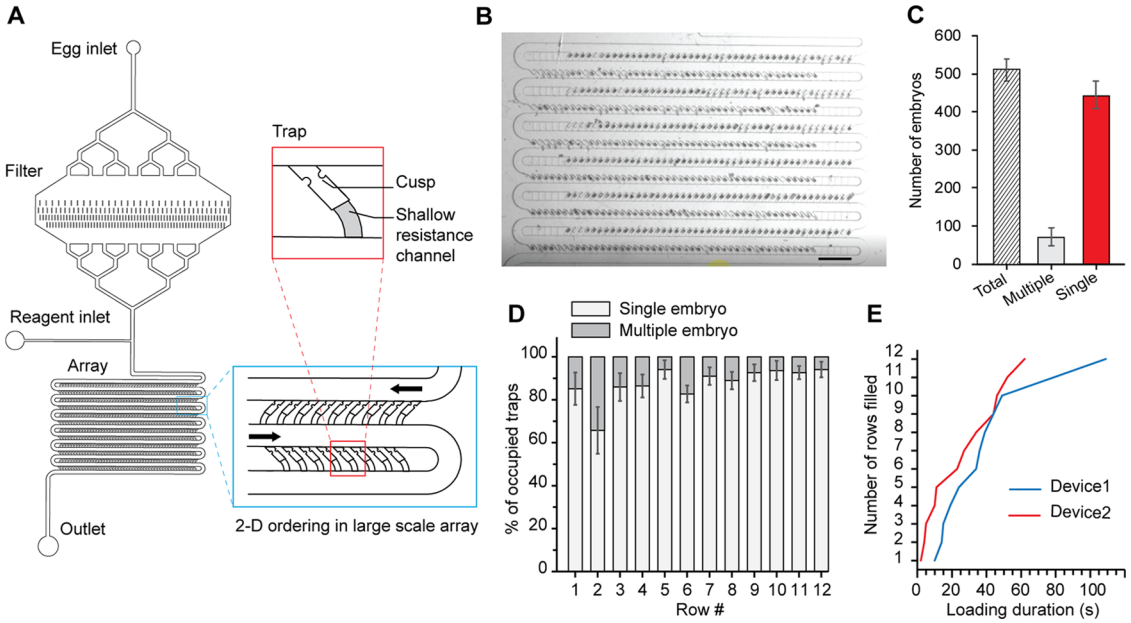

Figure 2. Microfluidic device design and loading characterization. (A) Schematic illustrating the device design and features incorporated to enable robust and reproducible hydrodynamic loading of hundreds of eggs (total trap number: 600) with the inset detailing the relevant geometrical dimensions; main channel (100 μm), trap size (35 μm), and resistance channel (12 μm). (B) Image of the microfluidic array showing single embryos loaded in the device in the AP direction (scale bar: 500 μm). (C) Quantification of loading occupancy in the device. (D) Homogeneity of egg loading throughout the array (c, d: n = 4 devices). Error bars represent SD. (E) Loading duration across two different devices.

However, such a requirement adds significantly to the difficulty of the task. To address this bottleneck, we designed a microfluidic array for capturing hundreds of *C. elegans* embryos. The system relies on hydrodynamic trapping, where embryos flowing through a main channel are drawn into bypass traps.[26−31] This design turns loading of the array into a deterministic process. As embryos flow in the channel, the embryos are drawn to the first available traps. Once trapped, the embryos obstruct the back-resistance channels, changing the flow streamline in the main serpentine channel. Therefore, the next coming embryos are drawn to the next available traps and this process repeats itself until complete filling of the array. This design allows for arraying embryos in high density and takes advantage of passive trapping to efficiently isolate single embryos from a bulk suspension (Figure 2A). To adapt this technology for large-scale phenotyping of gene expression using smFISH, several key aspects of the device design needed to be improved.

To allow for large-scale parallel mRNA counting with single-embryo resolution, we designed our microfluidic chip with several features specific to the smFISH application. First, to enable reagent delivery to all traps requires a clear flow path throughout the entire device. This is important as smFISH protocol involves multiple steps with different reagents. The challenge lies in how best to avoid embryos from clogging the channel because of their stickiness and natural tendency to clump together. Hence, to address this issue, we included an in-line filter and a second side inlet downstream the filter for reagent delivery. Upon embryo loading, the in-line filter reduces the number of embryo aggregates that reaches the array. Once loading is complete, the inclusion of the side inlet allows for injecting new reagents without pushing embryo aggregates trapped in the filter into the array (Figure 2A). Second, because we are interested in quantifying smFISH signals throughout the entire embryo sample, maximizing the imageable volume is important. Hence, we designed the traps to have the anterior−posterior (AP) axis horizontal, thus, ensuring that the z-direction depth only needs to be 30 μm and minimizing optical artifacts due to light scattering from the embryo tissue.

We demonstrate the efficient loading of hundreds of embryos in the A−P orientation and with a cleared main channel. Figure 2B shows an image of an array loaded with single embryos in the A−P axial orientation. Quantification of the loading occupancy across four devices shows reliable capture of more than 500 embryos per array (Figure 2C) and homogeneous distribution across the array (Figure 2D). Multiloading events were almost exclusively composed of n = 2 embryos. We observe less than 10% of empty traps. Small debris likely clogged the back-resistance channels of these traps, rendering them unavailable for embryos. Additional washing steps and/or use of gentler mechanical agitation and lower centrifugation speed during the egg preparation may help avoid debris and reduce the number of empty traps. In addition, the loading process is achieved within a couple of minutes: all 12 rows of the device are loaded in less than 2 minutes (Figure 2E and Supporting Video 1). The quick loading minimizes the amount of time the samples are exposed to formaldehyde, which can increase background fluorescence in the smFISH images. Altogether, these results demonstrate the ability of our microfluidic platform to capture hundreds of single embryos for downstream analysis.

Microfluidic Platform Enables Efficient Reagent Exchange Necessary for Executing smFISH Protocol. To execute smFISH protocol reproducibly on chip requires efficient reagent exchange. The smFISH protocol is a multistep process that involves several reagents, different concentrations, temperature changes, and incubation times. Proper execution of each step is important for obtaining quality smFISH images. However, while most of these parameters can be optimized by

https://dx.doi.org/10.1021/acs.analchem.0c02966
Anal. Chem. 2021, 93, 1369−1376

controlling external conditions, reagent delivery is achieved locally on-chip and is particularly sensitive. For example, delays in bringing the smFISH probe into and out of contact with the embryo can lead to lower probe concentration or overexposure resulting in lower smFISH signal, uneven staining, and high background fluorescence.[32,33] Reagent exchange is challenging because it requires delivering chemicals to the embryo without losing the embryo in the process. To solve this problem, we added two design considerations to address sample loss from the trap entrance or the back-channel. First, when moving the device from the cold room to the incubator or microscopy room, movement of the inlet and outlet tubing can generate fluctuations of pressure through the array and generate backflow. The back-pressure can push the embryo through the trap entrance in the main channel. This may result in sample loss when the flow is reapplied during the multistep protocol. To prevent that, we included a cusp at the trap entrance. The local narrowing of the channel maintains the embryo inside the trap.

Second, flow rates and viscous liquids (hybridization buffer viscosity is several tens of cP) induce shear forces that can push the embryo in or through the resistance channel. To solve this issue, we designed and compared the performances of three resistance channel geometries (Figure 3A and SI Figure 1). The first design is a single 12 × 26 μm^2 (width × height) channel. We hypothesized that creating a step-down (main channel height = 50 μm) would reinforce trapping efficiency. The second design is composed of two 13 × 12 μm^2 channels. Splitting the backflow channel may help with avoiding flow obstruction by the embryo and favor reagent exchange. The third design is similar to the first one but flipped into a single 26 × 12 μm^2 channel. This design reinforces the step-down effect. Despite their different geometry, all three designs have similar hydraulic resistance and lead to efficient embryo loading. However, we noticed undesirable effects for the first two designs. The first design failed to keep the embryo in the trap as the embryo fully blocks the flow and the pressure differential across the embryo pushes it partially or completely into the resistance channel. The second design prevents this issue as an embryo blocks only one of the two channels; however, the embryos were frequently morphologically distorted between the two resistance channels. Finally, the third design successfully achieves our goal. The shallow but wide resistance channel helps to prevent the embryo from entering the resistance channel while preserving its integrity, resulting in a low percentage of embryos being pushed into the resistance channel (<5%). Therefore, we selected this design for further characterization.

To ensure the device can exchange reagents efficiently without losing embryos, we studied the delivery of reagents in a fully loaded array device using fluorescein isothiocyanate (FITC)-dextran in hybridization buffer as a model for the smFISH probes. We measured FITC-dextran intensity at different locations in the device (Figure 3B) and showed that the fluorescence intensity increases over time and stabilizes in the device after roughly 30 s (Figure 3C), which is negligible compared to the duration of each step (30 min to several hours). To verify that reagent delivery is uniform over time, we compared the fluorescence intensity at the beginning of the assay (once the stable regime is reached) and 4 h later (~ duration of the probe hybridization step). Figure 3D shows that the measured FITC-dextran intensity in the device at the beginning of the experiment is close to the intensity at the end

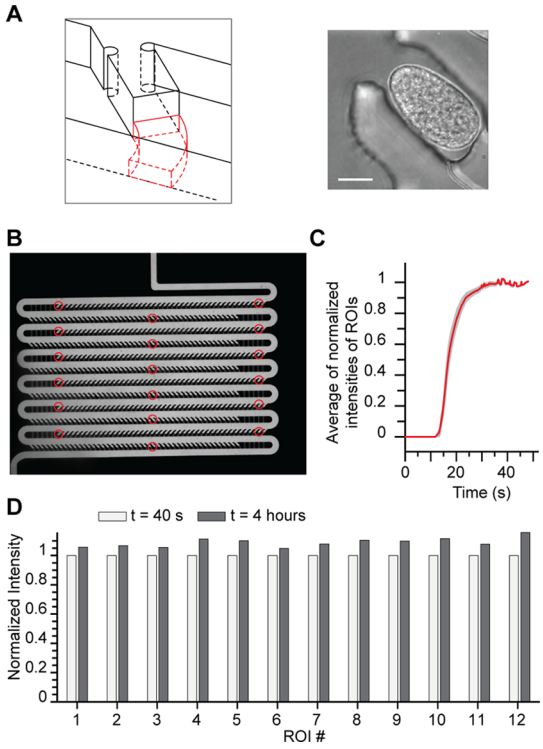

Figure 3. Device features enable efficient reagent exchange necessary for executing smFISH protocol. (A) Schematic of resistance channel geometry designed to maintain embryo positioning during smFISH protocol (left). Representative image of embryo trapped using the resistance channel geometry (right, scale bar: 15 μm). (B) Image of the device filled with FITC-dextran. ROIs analyzed are indicated by the red circles. (C) Plot describing the transition regimes for different ROIs throughout the array: delivery reaches rapid permanent regime after 30 seconds. Device was filled with wash buffer and exchanged with FITC-dextran in hybridization buffer to mimic the hybridization step of the smFISH experiment. (D) Bar graph of the average fluorescence intensity of the different ROIs in the device at the beginning (40 s) and end (4 h) of the mock hybridization experiment.

of the experiment and that these results are verified through the entire device. The small difference between the two time points can be explained by variation in the intensity of illumination. In summary, our on-chip protocol ensures efficient liquid exchange, which is essential for the proper execution of the complex multistep smFISH protocol.

On-Chip smFISH Staining Preserves Image Quality of Conventional Techniques. To check potential degradation in image quality that may arise from absorption of reagents in PDMS or optical artifact from PDMS walls, we compared smFISH assays performed in parallel on chip and off chip. Figure 4A shows representative fluorescence images. The embryos were hybridized with probes targeting mRNA transcripts of *par-1*, a kinase essential in early embryogenesis;[34,35] each spot indicates a single mRNA molecule, and the total number of punctae per embryo represents *par-1* transcript abundance. The presence of PDMS does not induce any artifact, and the overall image quality is preserved: we observe a homogeneous signal throughout the embryo and clear presence of punctae, typical of smFISH signal.[11] We quantified the signal-over-noise ratios (SNRs) to determine if the SNR of on-chip images is greater than 7, which is a requirement for smFISH image quantification as previously described.[24] The images of on-chip embryos have an SNR of

https://dx.doi.org/10.1021/acs.analchem.0c02966
Anal. Chem. 2021, 93, 1369−1376

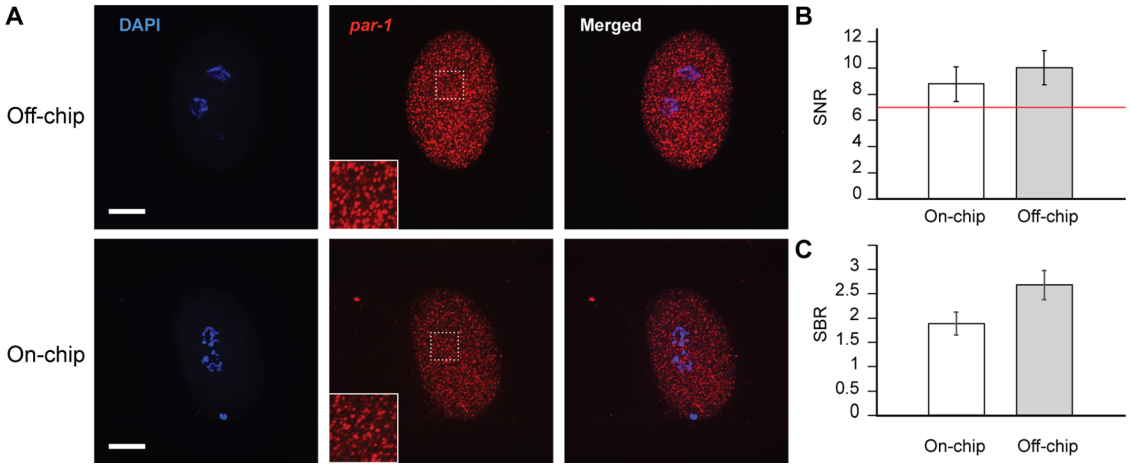

Figure 4. Comparison of on-chip smFISH protocol with the traditional off-chip method. (A) Representative images of eggs stained off-chip (top) and on-chip (bottom) with the smFISH protocol. Blue indicates DAPI and identifies nuclei by staining chromosomes. Red punctae indicate individual *par-1* molecules with zoom-in views in the insets. Scale bars are 15 μm. (B, C) Quantification of image quality between off-chip and on-chip experiments using SNR and SBR of the punctae for each condition. The red line indicates the minimum acceptable SNR for smFISH quantification (SNR = 7). Error bars represent SD, n = 20 embryos.

nearly 9, and the images of off-chip embryos have an SNR of 10 (Figure 4B). The slight difference between the two images may be reflective of lower intensity in the on-chip images as highlighted by the difference in signal-over-background ratios (SBRs) between the two methods (Figure 4C). Nonetheless, the SBR values are much greater than 1 and the SNR values are all above 7. Therefore, our method preserves the image quality necessary for performing valuable smFISH analysis.

Scaling-Up via Multiarray Integration. To study multiple conditions, it is necessary to scale up the device. For example, studies comparing different RNAi treatments or genotypes (natural variants or mutants) require batches of embryos to be assayed separately but otherwise identically. To do so, we integrated three devices and acquired smFISH images in a single session. Figure 5A shows representative images of *par-1* gene expression in embryos for each of the three devices. The images show similar and uniform quality across the embryos. We also calculated the signal-over-noise ratio to quantify signal quality and observe that the SNR values across the different devices are all over 7 and meet quality requirements for automated software analysis (Figure 5B).

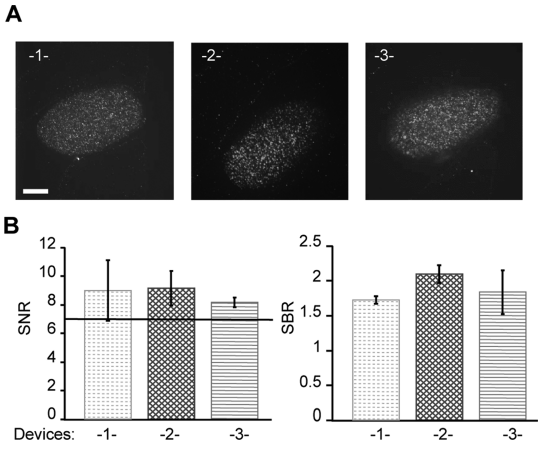

Figure 5. Integration of multiple arrays on a single substrate for high-throughput confocal imaging. (A) Representative smFISH images of embryos from each device. Red punctae indicate individual *par-1* molecules. Scale bar is 15 μm. (B) Quantification of image quality using SNR and SBR of punctae in each separate device. Error bars represent SD, n = 20 embryos.

These results also illustrate another critical advantage of our method, which is time-saving during image capture. Imaging with the traditional method remains time-consuming and labor-intensive because it requires tracking each embryo manually in bright field to register its position. Two bottlenecks render this process painstaking and inefficient. First, spotting embryos randomly spread on a large surface in the absence of any spatial marker is difficult. Second, throughput is limited by how many embryos are present on a single substrate. As one batch is processed, user input is necessary to remove the glass slide and mount another one on the microscope stage before repeating the process. Our microfluidic approach significantly improves these two bottlenecks. Arraying provides with a spatial frame to navigate through the samples and register their position. Furthermore, the small footprint of a single array allows for the integration of multiple arrays on a single glass slide. Therefore, the embryo-position registration can be done at once; the continuous presence of an operator is no more mandatory to image hundreds of samples. For example, using a traditional approach would require imaging 30 coverslips to image 60 embryos of a developmental stage. With our microfluidics-based approach, this type of analysis would require only three devices saving time and labor. Scaling-up via multiarray integration does not compromise experimental integrity, affording a dramatic increase in sample size and image efficiency while eliminating potential batch effects across treatments. This benefit could be exploited further, limited only by the number of devices that can be arranged on a slide.

Highly Resolved Temporal Analysis of Gene Expression Using Microfluidic Platform. Obtaining a detailed temporal analysis of the RNA levels in an organism is key to understanding the effect of its genotype on its traits and behavior.[36] This knowledge will not only provide information about gene expression dynamics in tissues of interest but also provide insight into gene interactions that occur throughout the organism's life cycle.[37] To demonstrate the ability to assay embryos across developmental stages at high temporal

https://dx.doi.org/10.1021/acs.analchem.0c02966
Anal. Chem. 2021, 93, 1369−1376

resolution, we freeze-cracked, arrayed, and stained embryos on-chip with the nuclei stain DAPI. In addition, using the *par-1* gene as a case study, we demonstrate that the platform can provide information on the dynamics of gene expression during embryogenesis. *par-1* plays a key role in the asymmetric division during early developmental events.[38−40] Therefore, we imaged and quantified gene expression of developmental stages ranging from just before the first cleavage (2-cell stage) to the beginning of gastrulation (30-cell stage).

We observe a decline in *par-1* gene expression between early developmental stages and later time points (Figure 6). This

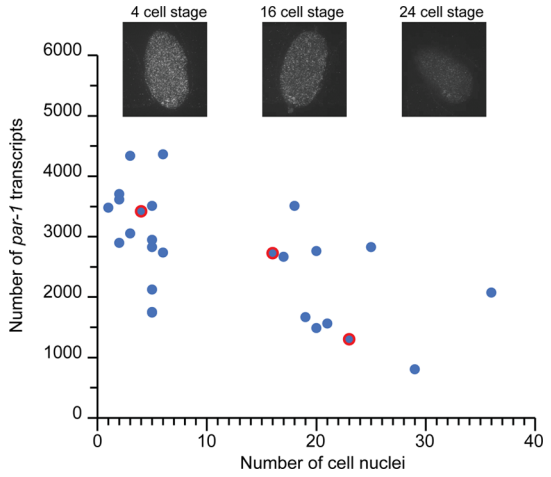

Figure 6. Time-resolved analysis of *par-1* gene expression changes during early embryogenesis showing the transcript count versus number of cell nuclei (n = 25 embryos). The insets show representative smFISH images of embryos at different developmental stages corresponding to the red-circled data points.

observation is consistent with the known essential activity of PAR-1 during embryonic polarization[34,35] as well as observations of declining *par-1* transcripts at later stages.[41] This observation is also consistent with our own measurements using the traditional off-chip method (SI Figure 2). With a similar trend to our on-chip samples, the number of *par-1* gene transcripts declined from 4,000 transcripts at the 2−4-cell stage to 1,500 transcripts at 30-cell stage. Altogether, these results highlight the performance and utility of our platform to advance biological studies requiring longitudinal data about gene expression at a high temporal resolution. It is interesting to note that, during the embryo-collecting process, embryos as old as mid-gastrulation (~150-cell stage) were also collected (but not analyzed). Since embryos do not change size during development, our device can be used to perform longitudinal studies of gene expression at later stages during the proliferation, metamorphosis, elongation, and quickening phases.

CONCLUSIONS

In this study, we report the development of a microfluidics-based smFISH method, which we use to demonstrate changing gene expression in *C. elegans* embryogenesis at high temporal resolution. We designed a large-capacity, high-density array that can load hundreds of embryos in a few tens of seconds. By trapping large numbers of embryos, this method enables study designs that require large sample sizes, for example, assays of changing gene expression across developmental stages. The trap geometry promotes efficient reagent exchange, which allows wash, hybridization, staining, and related steps to be performed on-chip. Finally, the small device footprint allows for multiarray integration that facilitates image acquisition and allows for the application of our platform to larger-scale studies. Our approach for reagent delivery and exchange not only reduces the labor-intensiveness of the smFISH protocol but also allows for the integration of alternative or additional assays, such as immunostaining. Further, because the design principles used are not specific to the exact dimensions of *C. elegans* embryos, simple scaling should allow our approach to be adapted for other problems, including development and pathogenesis in *Drosophila* or other small genetic model organisms, cancer spheroids, stem cell aggregates, or organoids.

In modern biology, limits to experimental or statistical power often constrain elucidation of the molecular and cellular dynamics that govern development or the relationship between genotype and phenotype. For example, just as large sample sizes are required to measure change across developmental time, high replication is often required to detect differences in trait expression between multiple genotypes. By enabling loading, staining, washing, and other reagent exchange steps for hundreds of embryos and by minimizing user effort during image capture, this method offers a generalizable way to scale up the use of molecular tools routinely used in developmental genetics research to address larger questions at the level of the biological system.

ASSOCIATED CONTENT

Supporting Information

The Supporting Information is available free of charge at https://pubs.acs.org/doi/10.1021/acs.analchem.0c02966.

Results, including schematics and pictures of microfluidic trapping chambers and *par-1* gene expression obtained via the traditional off-chip method (PDF)

Results, including the movie of array loading with *C. elegans* embryos (MP4)

AUTHOR INFORMATION

Corresponding Author

Hang Lu − *Wallace H. Coulter Department of Biomedical Engineering, Interdisciplinary Program in Bioengineering, and School of Chemical & Biomolecular Engineering, Georgia Institute of Technology, Atlanta, Georgia 30332, United States;* orcid.org/0000-0002-6881-660X; Email: hang.lu@gatech.edu

Authors

Seleipiri Charles − *Wallace H. Coulter Department of Biomedical Engineering and Interdisciplinary Program in Bioengineering, Georgia Institute of Technology, Atlanta, Georgia 30332, United States*

Guillaume Aubry − *School of Chemical & Biomolecular Engineering, Georgia Institute of Technology, Atlanta, Georgia 30332, United States*

Han-Ting Chou − *School of Biological Sciences, Georgia Institute of Technology, Atlanta, Georgia 30332, United States;* orcid.org/0000-0002-1259-2694

Annalise B. Paaby − *School of Biological Sciences, Georgia Institute of Technology, Atlanta, Georgia 30332, United States*

Complete contact information is available at:

https://dx.doi.org/10.1021/acs.analchem.0c02966
Anal. Chem. 2021, 93, 1369−1376

https://pubs.acs.org/10.1021/acs.analchem.0c02966

Author Contributions

⊥S.C. and G.A. contributed equally to this work.

Notes

The authors declare no competing financial interest.

■ ACKNOWLEDGMENTS

The authors acknowledge funding from the National Institutes of Health, National Science Foundation, Simons Foundation, and Marcus Foundation (NIH R01NS115484, R01AG056436, R01NS096581, R01GM088333, NSF 1764406, 1707401, and 0939511, Simons Foundation, Marcus Center for Therapeutic Cell Characterization and Manufacturing grants to H.L., NIH R35 GM119744 to A.B.P., NIH R21NS117066 to H.L. and G.A.). The authors also thank A. Lifland for his technical assistance and Drs. G. Sun, M. Crane, and D. Patel for their inputs on the manuscript.

■ REFERENCES

(1) Wood, W. B. *The Nematode Caenorhabditis elegans*; Cold Spring Harbor Laboratory: New York, 1988.
(2) Bryson-Richardson, R.; Berger, S.; Currie, P. *Atlas of Zebrafish Development*; Academic Press: San Diego, 2012.
(3) Bate, M.; Martinez Arias, A. *The Development of Drosophila melanogaster*; Cold Spring Harbor Laboratory: New York, 1993.
(4) Raj, A.; Rifkin, S. A.; Andersen, E.; van Oudenaarden, A. *Nature* **2010**, *463*, 913−918.
(5) Kistler, K. E.; Trcek, T.; Hurd, T. R.; Chen, R.; Liang, F.-X.; Sall, J.; Kato, M.; Lehmann, R. *eLife* **2018**, *7*, No. e37949.
(6) Rahimi, N.; Carmon, S.; Averbukh, I.; Khajouei, F.; Sinha, S.; Schejter, E. D.; Barkai, N.; Shilo, B.-Z. *Proc. Natl. Acad. Sci. U.S.A.* **2020**, *117*, 1552−1558.
(7) Couturier, L.; Mazouni, K.; Corson, F.; Schweisguth, F. *Nat. Commun.* **2019**, *10*, No. 3486.
(8) York, A. G.; Chandris, P.; Nogare, D. D.; Head, J.; Wawrzusin, P.; Fischer, R. S.; Chitnis, A.; Shroff, H. *Nat. Methods* **2013**, *10*, 1122−1126.
(9) Port, F.; Chen, H.-M.; Lee, T.; Bullock, S. L. *Proc. Natl. Acad. Sci. U.S.A.* **2014**, *111*, E2967−E2976.
(10) Ji, N.; van Oudenaarden, A. *WormBook* **2012**, 1−16.
(11) Raj, A.; van den Bogaard, P.; Rifkin, S. A.; van Oudenaarden, A.; Tyagi, S. *Nat. Methods* **2008**, *5*, 877−879.
(12) Chen, K. H.; Boettiger, A. N.; Moffitt, J. R.; Wang, S.; Zhuang, X. *Science* **2015**, *348*, No. aaa6090.
(13) Eng, C.-H. L.; Lawson, M.; Zhu, Q.; Dries, R.; Koulena, N.; Takei, Y.; Yun, J.; Cronin, C.; Karp, C.; Yuan, G.-C.; Cai, L. *Nature* **2019**, *568*, 235−239.
(14) Shaffer, S. M.; Wu, M. T.; Levesque, M. J.; Raj, A. *PLoS One* **2013**, *8*, No. e75120.
(15) Goh, J. J. L.; Chou, N.; Seow, W. Y.; Ha, N.; Cheng, C. P. P.; Chang, Y.-C.; Zhao, Z. W.; Chen, K. H. *Nat. Methods* **2020**, *17*, 689−693.
(16) Rouhanifard, S. H.; Mellis, I. A.; Dunagin, M.; Bayatpour, S.; Jiang, C. L.; Dardani, I.; Symmons, O.; Emert, B.; Torre, E.; Cote, A.; Sullivan, A.; Stamatoyannopoulos, J. A.; Raj, A. *Nat. Biotechnol.* **2019**, *37*, 84−89.
(17) Kishi, J. Y.; Lapan, S. W.; Beliveau, B. J.; West, E. R.; Zhu, A.; Sasaki, H. M.; Saka, S. K.; Wang, Y.; Cepko, C. L.; Yin, P. *Nat. Methods* **2019**, *16*, 533−544.
(18) Atakan, H. B.; Xiang, R.; Cornaglia, M.; Mouchiroud, L.; Katsyuba, E.; Auwerx, J.; Gijs, M. A. M. *Sci. Rep.* **2019**, *9*, No. 14340.
(19) Cornaglia, M.; Lehnert, T.; Gijs, M. A. M. *Lab Chip* **2017**, *17*, 3736−3759.
(20) Cornaglia, M.; Mouchiroud, L.; Marette, A.; Narasimhan, S.; Lehnert, T.; Jovaisaite, V.; Auwerx, J.; Gijs, M. A. M. *Sci. Rep.* **2015**, *5*, No. 10192.
(21) Dong, L.; Jankele, R.; Cornaglia, M.; Lehnert, T.; Gonczy, P.; Gijs, M. A. M. *Adv. Sci.* **2018**, *5*, No. 1700751.
(22) Duffy, D. C.; McDonald, J. C.; Schueller, O. J.; Whitesides, G. M. *Anal. Chem.* **1998**, *70*, 4974−4984.
(23) Stiernagle, T. Maintenance of *C. elegans The C. elegans Research Community*, 2006, DOI: 10.1895/wormbook.1.101.1.
(24) Mueller, F.; Senecal, A.; Tantale, K.; Marie-Nelly, H.; Ly, N.; Collin, O.; Basyuk, E.; Bertrand, E.; Darzacq, X.; Zimmer, C. *Nat. Methods* **2013**, *10*, 277−278.
(25) Hall, D. H.; Herndon, L. A.; Altun, Z. Introduction to *C. elegans* embryo *WormAtlas* 2017, DOI: 10.3908/wormatlas.4.1.
(26) Goyal, Y.; Levario, T. J.; Mattingly, H. H.; Holmes, S.; Shvartsman, S. Y.; Lu, H. *Dis. Model. Mech.* **2017**, *10*, 923−929.
(27) Levario, T. J.; Zhan, M.; Lim, B.; Shvartsman, S. Y.; Lu, H. *Nat. Protoc.* **2013**, *8*, 721−736.
(28) Jackson-Holmes, E. L.; McDevitt, T. C.; Lu, H. *Lab Chip* **2017**, *17*, 3634−3642.
(29) Chung, K.; Kim, Y.; Kanodia, J. S.; Gong, E.; Shvartsman, S. Y.; Lu, H. *Nat. Methods* **2011**, *8*, 171−U103.
(30) Chung, K.; Rivet, C. A.; Kemp, M. L.; Lu, H. *Anal. Chem.* **2011**, *83*, 7044−7052.
(31) Lee, H.; Kim, S. A.; Coakley, S.; Mugno, P.; Hammarlund, M.; Hilliard, M. A.; Lu, H. *Lab Chip* **2014**, *14*, 4513−4522.
(32) Ostromohov, N.; Huber, D.; Bercovici, M.; Kaigala, G. V. *Anal. Chem.* **2018**, *90*, 11470−11477.
(33) Sun, G.; Wan, J.; Lu, H. *Biomicrofluidics* **2019**, *13*, No. 064101.
(34) Folkmann, A. W.; Seydoux, G. *Development* **2019**, *146*, No. dev171116.
(35) Kemphues, K. J.; Priess, J. R.; Morton, D. G.; Cheng, N. S. *Cell* **1988**, *52*, 311−320.
(36) Boeck, M. E.; Huynh, C.; Gevirtzman, L.; Thompson, O. A.; Wang, G.; Kasper, D. M.; Reinke, V.; Hillier, L. W.; Waterston, R. H. *Genome Res.* **2016**, *26*, 1441−1450.
(37) Packer, J. S.; Zhu, Q.; Huynh, C.; Sivaramakrishnan, P.; Preston, E.; Dueck, H.; Stefanik, D.; Tan, K.; Trapnell, C.; Kim, J.; Waterston, R. H.; Murray, J. I. *Science* **2019**, *365*, No. eaax1971.
(38) Guo, S.; Kemphues, K. *Cell* **1995**, *81*, 611−620.
(39) Suzuki, A. *Cell Polarity 1: Biological Role and Basic Mechanisms*; Ebnet, K., Ed.; Springer International Publishing: Cham, 2015; pp 25−50.
(40) Wu, Y.; Griffin, E. E. *Curr. Top. Dev. Biol.* **2017**, *123*, 365−397.
(41) Levin, M.; Hashimshony, T.; Wagner, F.; Yanai, I. *Dev. Cell* **2012**, *22*, 1101−1108.